CHEMISTRY
AN ASIAN JOURNAL

DOI: 10.1002/asia.200900362

Binuclear Ni^{II}-DpaTyr Complex as a High Affinity Probe for an Oligo-Aspartate Tag Tethered to Proteins

Akio Ojida,[a, b] Sho-hei Fujishima,[a] Kei Honda,[a] Hiroshi Nonaka,[a] Sho-hei Uchinomiya,[a] and Itaru Hamachi*[a, c]

Abstract: A complementary recognition pair of a short-peptide tag and a small molecular probe is a versatile molecular tool for protein detection, handling, and purification, and so forth. In this manuscript, we report that the binuclear Ni^{II}-DpaTyr (DpaTyr = bis((dipicolylamino)methyl)-tyrosine) complex serves as a strong binding probe for an oligo-aspartate tag tethered to a protein. Among various binuclear metal complexes of M-DpaTyr (M = Zn^{II}, Ni^{II}, Mn^{II}, Cu^{II}, Cd^{II}, Co^{III}, and Fe^{III}), we have found that Ni^{II}-DpaTyr (**1**-2Ni^{II}) displays a strong-binding affinity (apparent binding constant: $K_{app} \approx 10^5\,M^{-1}$) for an oligo-aspartate peptide under neutral aqueous conditions (50 mM HEPES, 100 mM NaCl, pH 7.2). Detailed isothermal-titration calorimetry (ITC) studies reveal that the tri-aspartate D3-tag (DDD) is an optimal sequence recognized by **1**-2Ni^{II} in a 1:1 binding stoichiometry. On the other hand, other metal complexes of DpaTyr, except for Ni^{II}- and Zn^{II}-DpaTyr, show a negligible binding affinity for the oligo-aspartate peptide. The binding affinity was greatly enhanced in the pair between the dimer of Ni^{II}-DpaTyr and the repeated D3 tag peptide (D3×2), such as DDDXXDDD, on the basis of the multivalent coordination interaction between them. Most notably, a remarkably high-binding affinity ($K_{app} = 2 \times 10^9\,M^{-1}$) was achieved between the Ni^{II}-DpaTyr dimer **4**-4Ni^{II} and the D3×2 tag peptide (DDDNGDDD). This affinity is ≈100-fold stronger than that observed in the binding pair of the Zn^{II}-DpaTyr (**4**-4Zn^{II}) and the D4×2 tag (DDDDGDDDD), a useful tag-probe pair previously reported by us. The recognition pair of the Ni^{II}-DpaTyr probe and the D3×2 tag can also work effectively on a protein surface, that is, **4**-4Ni^{II} is strongly bound to the FKBP12 protein tethered with the D3×2 tag (DDDNGDDD) with a large K_{app} value of $5 \times 10^8\,M^{-1}$. Taking advantage of the strong-binding affinity, this pair was successfully applied to the selective inactivation of the tag-fused β-galactosidase by using the chromophore-assisted light inactivation (CALI) technique under crude conditions, such as cell lysate.

Keywords: molecular recognition · peptides · probe · proteins

Introduction

Molecular recognition of proteins with small molecules has long been a central interest for protein researchers. Regardless of their biological activities, the small molecular probes with a strong and selective binding affinity for a certain protein are useful as a versatile molecular tool in a wide range of protein research. For example, biotin is well known as a specific ligand for (strept)avidin with an extremely strong-binding affinity (apparent binding constant: $K_{app} \approx 10^{15}\,M^{-1}$), so that this recognition pair is now widely used as an invaluable tool in detection, isolation, as well as immobilization of proteins.[1] Other specific binding pairs, which include methotrexate and DHFR (dihydrofolate reductase),[2] and rapamycin and FKBP (FK506 binding protein) or FRB (FKBP-rapamycin binding protein),[3] have also been used for selective protein labeling and function analyses of cells.

[a] Dr. A. Ojida, S.-h. Fujishima, Dr. K. Honda, H. Nonaka, S.-h. Uchinomiya, Prof. I. Hamachi
Department of Synthetic Chemistry and Biological Chemistry
Graduate School of Engineering
Kyoto University
Katsura Campus, Nishikyo-ku, Kyoto, 615-8510 (Japan)
Fax: (+81) 75-383-2759
E-mail: ihamachi@sbchem.kyoto-u.ac.jp

[b] Dr. A. Ojida
JST, PRESTO (Life Phenomena and Measurement Analysis)
Sanbancho, Chiyodaku, Tokyo, 102-0075 (Japan)

[c] Prof. I. Hamachi
JST, CREST (Creation of Next-generation Nanosystems through Process Integration)
Sanbancho, Chiyodaku, Tokyo, 102-0075 (Japan)

Supporting information for this article is available on the WWW under http://dx.doi.org/10.1002/asia.200900362.

A complementary recognition pair consisting of a small molecular probe and a short-peptide tag is an artificial recognition system to realize a desirable specific binding with a protein of interest. In contrast to the binding systems employing the above-mentioned natural proteins, the artificial tag-probe system is generally useful to achieve a specific binding just by genetically incorporating a short-peptide tag into a target protein with minimal perturbation of protein functions, owing to its small size. Owing to these general utilities and advantages, several tag-probe pairs have been developed as a tool to facilitate protein research.[4] A representative pair of Ni^{II}-NTA (nitrilotriacetic acid) and oligohistidine tag (His-tag)[5] is now available for protein purification by using affinity-column chromatography, protein immobilization on a microtiter plate, as well as cell-bioimaging study by using fluorescence microscopy.[6] However, despite the apparent versatility, available complementary tag-probe pairs are still limited, mainly owing to the general difficulty in de novo design of a molecular recognition system composed with a small molecular probe and a short-peptide tag. Therefore, it is a challenging task in the field of molecular recognition to develop a new tag-probe pair with a high specificity, as well as an orthogonality against other protein recognition systems, which would contribute to expand the versatility of the tag-probe system and provide a molecular tool useful for protein analysis and engineering.[7]

We have recently reported that the binuclear Zn^{II}-complex **1**-2Zn^{II} (Zn^{II}-DpaTyr, (DpaTyr = bis((dipicolylamino)-methyl)tyrosine), Figure 1) serves as a specific binding probe for a tetra-aspartate peptide tag (DDDD, D4-tag) under the neutral aqueous conditions.[8] Based on this finding, a strong-binding affinity ($K_{app} = 1.8 \times 10^7\ M^{-1}$) was achieved in the pair between Zn^{II}-DpaTyr dimer such as **4**-4Zn^{II} and a D4×2 (DDDDGDDDD) tag-fused protein, so that this tag-probe pair was successfully applied for the fluorescence imaging of a protein on a living-cell surface.[8a] In this manuscript, we describe a new molecular recognition pair composed of the Ni^{II}-complex of DpaTyr (Ni^{II}-DpaTyr) and an oligo-aspartate tag. Among various metal complexes of DpaTyrs, we found that Ni-(II)-DpaTyr **1**-2Ni^{II} serves as an effective binding probe for the tri-aspartate tag (DDD, D3-tag). Most interestingly, the dimer of Ni^{II}-DpaTyr (**4**-4Ni^{II}) showed a remarkably strong-binding affinity ($K_{app} = 2.0 \times 10^9\ M^{-1}$) for a short D3×2 tag peptide (DDDNGDDD), the value of which is ≈100-fold larger than that of the previous tag-probe pair of **4**-4Zn^{II} and D4×2 tag ($K_{app} = 1.8 \times 10^7\ M^{-1}$). Taking advantage of the strong binding of Ni^{II}-DpaTyr, we successfully applied this pair for the selective deactivation of D3×2 tag-fused β-galactosidase by using the CALI (chromophore-assisted light inactivation) technique under crude conditions, such as in the cell lysate of *E. coli*.

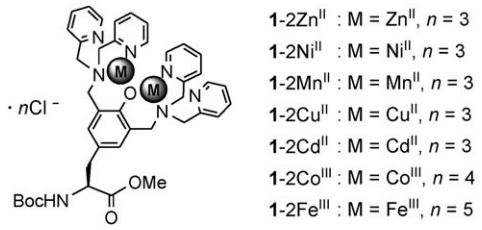

1-2Zn^{II} : M = Zn^{II}, *n* = 3
1-2Ni^{II} : M = Ni^{II}, *n* = 3
1-2Mn^{II} : M = Mn^{II}, *n* = 3
1-2Cu^{II} : M = Cu^{II}, *n* = 3
1-2Cd^{II} : M = Cd^{II}, *n* = 3
1-2Co^{III} : M = Co^{III}, *n* = 4
1-2Fe^{III} : M = Fe^{III}, *n* = 5

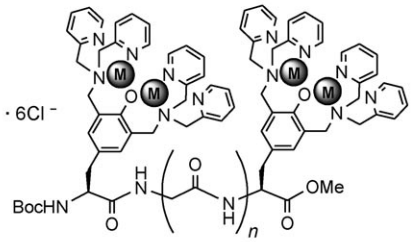

2-4Ni^{II} : M = Ni^{II}, *n* = 0
3-4Ni^{II} : M = Ni^{II}, *n* = 1
4-4Ni^{II} : M = Ni^{II}, *n* = 2
4-4Zn^{II}: M = Zn^{II}, *n* = 2

Figure 1. Molecular structures of the synthetic metal-DpaTyr complexes.

Results and Discussion

Evaluation of the Binding Affinity of the Metal-DpaTyrs toward Oligo-Aspartate Peptide

To perform screening of a metal complex that displays a strong-binding affinity towards an oligo-aspartate peptide, we initially prepared a series of the binuclear metal complexes of the DpaTyr **1**-2M (M = Zn^{II}, Ni^{II}, Mn^{II}, Cu^{II}, Cd^{II}, Co^{III}, and Fe^{III}, Figure 1) and evaluated their binding affinities for the tetra-aspartate D4 peptide (Boc-DDDD-NH_2) by isothermal-titration calorimetry (ITC). The results of the ITC experiments are summarized in Table 1. We previously revealed, by means of an ITC study, that **1**-2Zn^{II} binds to the D4 peptide with a moderate-binding affinity ($4.87 \pm 0.13 \times 10^4\ M^{-1}$, $n = 0.76$) under neutral aqueous conditions (50 mM HEPES, 100 mM NaCl, pH 7.2) through an exothermic binding process ($\Delta H = -5.10 \pm 0.11$ kcal mol^{-1}, $T\Delta S = 1.30$ kcal mol^{-1}, (Figure 2).[8a] Among the other metal complexes, we have found that **1**-2Ni^{II} is able to interact with the D4 peptide through an endothermic entropy driven process ($\Delta H = 6.18 \pm 0.09$ kcal mol^{-1}, $T\Delta S = 13.96$ kcal mol^{-1})

Table 1. Summary of the ITC titration experiments between various metal complexes of DpaTyr **1**-2M and D4 peptide.[a,b,c]

	1-2Zn^{II}	**1**-2Ni^{II}	**1**-2Mn^{II}	**1**-2Cu^{II}	**1**-2Cd^{II}	**1**-2Co^{III}	**1**-2Fe^{III}
n	0.76±0.01	0.53±0.06					
K_{app}	(4.87±0.13)×10^4	(5.18±0.41)×10^5	<10^3	<10^3	<10^3	<10^3	<10^3
ΔH	−5.10±0.11	6.18±0.09	–[d]	–[d]	–[d]	–[d]	–[d]
$T\Delta S$	1.30	13.96					

[a] *n* = stoichiometry, K_{app} = binding constant (M^{-1}), ΔH = enthalpy (kcal mol^{-1}), $T\Delta S$ = entropy (kcal mol^{-1}). [b] D4 peptide = Boc-$(Asp)_4$-NH_2. [c] Measurement conditions: [**1**-2M] = 50 μM, 50 mM HEPES, 100 mM NaCl, pH 7.2, 25 °C. [d] Heat formation was scarcely detected.

with a large K_{app} value of $5.18 \pm 0.41 \times 10^5\,M^{-1}$, although their binding stoichiometry is apparently not 1:1 ($n = 0.53$). On the other hand, negligible heat formation was observed in the titration of other metal complexes, such as **1**-2Mn^{II}, **1**-2Cu^{II}, **1**-2Cd^{II}-, **1**-2Co^{III}-, and **1**-2Fe^{III}, indicating that their binding affinities for the D4 peptide are very weak ($K_{app} < 10^3\,M^{-1}$). This screening suggested that **1**-2Ni^{II} is a promising new metal complex as a probe for the oligo-aspartate tag with a potentially strong-binding affinity.

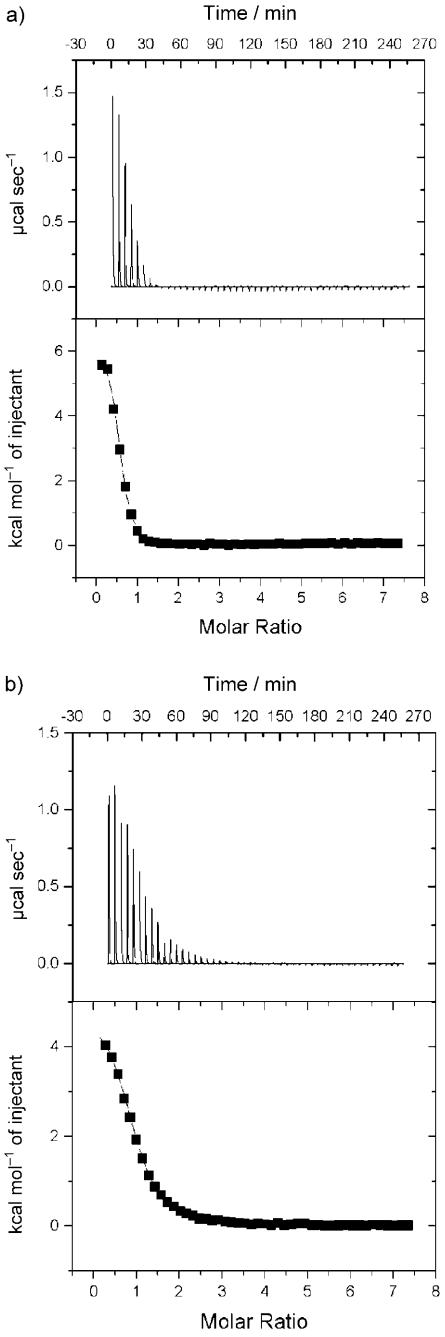

Figure 2. ITC titration curve (upper) and processed data (lower) in the titration of **1**-2Ni^{II} with a) D4 peptide and b) D3 peptide. Measurement conditions: [**1**-2Ni^{II}] = 50 µM, [D4 or D3] = 2 mM (5 µL × 48 injections), 50 mM HEPES, 100 mM NaCl, pH 7.2, 25 °C.

The binding property of **1**-2Ni^{II} was further evaluated by the ITC measurements with a series of the oligo-aspartate peptides. These data are summarized in Table 2, which also includes the binding data of **1**-2Zn^{II} for comparison. We found that **1**-2Ni^{II} displays a 1:1 binding stoichiometry ($n = 0.91$) for D3 peptide (DDD), wherein the binding affinity ($K_{app} = 1.5 \times 10^5\,M^{-1}$) is larger by ≈20- and 3-fold than the corresponding binding pair of **1**-2Zn^{II} with D3 ($K_{app} = 8.54 \times 10^3\,M^{-1}$, $n = 0.93$) and D4 peptide ($K_{app} = 4.87 \times 10^4\,M^{-1}$, $n = 0.76$), respectively. The binding affinities of **1**-2Ni^{II} with the other tri-aspartate peptides (DDD, DADD, DDAD) were greater than those with the di-aspartate peptides (DD, DAD, and DAAD), in all cases the binding stoichiometry was evaluated to be 1:1 ($n = 0.83$–1.07). Given the data that the binding stoichiometry of **1**-2Ni^{II} with the tetra-aspartate D4 peptide was estimated to be 2:1 ($n = 0.51$, Table 1), we can conclude that **1**-2Ni^{II} interacts with up to three aspartate residues in a short oligo-aspartate peptide.[9] The ITC data also revealed that the interaction of **1**-2Ni^{II} with the oligo-aspartate peptides is an endothermic entropy driven process ($\Delta H > 0$, $T\Delta S > 0$) in all the cases. This is a good contrast to the results of Zn^{II}-DpaTyr for which the binding to the oligo-aspartate peptides is an exothermic process ($\Delta H < 0$, Tables 1 and 2). These results imply that the binding of **1**-2Ni^{II} involves a larger number of the released hydration waters compared to the case of **1**-2Zn^{II}, so that the positive enthalpy change was induced, which is in turn favorably compensated by the positive entropy change in the binding processes.[10]

The binding selectivity of **1**-2Ni^{II} was also evaluated by using ITC experiments with other peptides and biological relevant anions (Table 3). We found that the binding of **1**-2Ni^{II} to His-tag peptide (His6; HHHHHH) was very weak ($K_{app} < 10^3\,M^{-1}$).[5] Since significant interaction was not also observed between the oligo-aspartate peptide and Ni^{II}-NTA,[8a] the D3 tag/Ni^{II}-DpaTyr pair is orthogonal to the conventional His tag/Ni^{II}-NTA pair. **1**-2Ni^{II} was able to bind to E3 peptide (EEE) with a moderate binding affinity ($K_{app} = 1.8 \times 10^4\,M^{-1}$). However, this binding is weaker by ≈10-fold than the corresponding binding with D3 tag ($K_{app} = 1.5 \times 10^5\,M^{-1}$), indicating that D3 tag is better than E3 tag. We also found that the binding affinity of **1**-2Ni^{II} with the biological relevant anions, such as inorganic phosphate and sulfate is negligible ($K_{app} < 10^3\,M^{-1}$). These results suggest that **1**-2Ni^{II} not only strongly binds to D3 tag, but also has a sufficient binding selectivity among the biological substances.

Enhancement of the Binding Affinity by Multivalent Binding Effect

The exploitation of multivalent binding is an effective strategy to enhance the binding affinity of a recognition pair.[11] On the basis of this strategy, we designed several dimers of the Ni^{II}-DpaTyr complex, **2**-4Ni^{II}, **3**-4Ni^{II}, and **4**-4Ni^{II}, which possess a different number of glycine linker units ($n = 0$–2, Figure 1). We evaluated their binding affinities for the three

Table 2. Summary of the ITC titration experiments of **1**-2Ni^{II} or **1**-2Zn^{II} with various oligo-aspartate peptides.[a,b,c]

		DDD (D3)	DADD	DDAD	DD	DAD	DAAD
1-2Ni^{II}	n	0.91±0.01	0.83±0.01	0.84±0.00	0.96±0.06	0.91±0.01	1.07±0.24
	K_{app}	(1.56±0.05)×10^5	(7.80±0.22)×10^4	(3.37±0.06)×10^5	(9.43±0.25)×10^3	(5.88±0.15)×10^4	(6.32±0.47)×10^3
	ΔH	4.91±0.05	6.80±0.01	4.60±0.02	5.81±0.41	5.90±0.09	3.15±0.76
	$T\Delta S$	11.98	13.46	12.1	11.22	12.40	8.33
1-2Zn^{II}	n	0.93±0.10					
	K_{app}	(8.54±0.36)×10^3					
	ΔH	−3.75±0.43	_[d]	_[d]	_[d]	_[d]	_[d]
	$T\Delta S$	1.61					

[a] n = stoichiometry, K_{app} = binding constant (M^{-1}), ΔH = enthalpy (kcal mol^{-1}), $T\Delta S$ = entropy (kcal mol^{-1}). [b] DDD (D3) = Boc-(Asp)$_3$-NH$_2$, DADD = Boc-Asp-Ala-Asp-Asp-NH$_2$, DDAD = Boc-Asp-Asp-Ala-Asp-NH$_2$, DD = Boc-Asp-Asp-NH$_2$, DAD = Boc-Asp-Ala-Asp-NH$_2$, DAAD = Boc-Asp-Ala-Ala-Asp-NH$_2$. [c] Measurement conditions: [**1**-2Ni^{II}] = 50 μM, 50 mM HEPES, 100 mM NaCl, pH 7.2, 25 °C. [d] Not measured.

Table 3. Summary of the ITC titration experiments of **1**-2Ni^{II} with various peptides and anions.[a,b]

	HHHHHH[c] (His6)	EEE[c] (Glu3)	Na_2SO4[d]	Na_2HPO_4[d]
n		1.11±0.07		
K_{app}	$<10^3$	(1.77±0.11)×10^4	$<10^3$	$<10^3$
ΔH	_[e]	4.17±0.29	_[e]	_[e]
$T\Delta S$		9.96		

[a] n = stoichiometry, K_{app} = binding constant (M^{-1}), ΔH = enthalpy (kcal mol^{-1}), $T\Delta S$ = entropy (kcal mol^{-1}). [b] HHHHHH (His6) = Ac-Tyr-(His)$_6$-NH$_2$, EEE = Boc-(Glu)$_3$-NH$_2$, [c] Measurement conditions: [**1**-2Ni^{II}] = 50 μM, 50 mM HEPES, 100 mM NaCl, pH 7.2, 25 °C. [d] Measurement conditions: [**1**-2Ni^{II}] = 50 μM, 50 mM Tris-HCl, 100 mM NaCl, pH 7.2, 25 °C. [e] Heat formation was barely detected.

types of the poly-aspartate D3×2 peptides composed of the repeated D3 units (DDD-XX-DDD, XX = AA, PG, or NG). The synthesis and characterization of the Ni^{II} complexes are described in Figure S1 in the Supporting Information. It is well known that paramagnetic Ni^{II} complexes display a strong fluorescence quenching effect.[12] Thus, we evaluated the binding affinity between the Ni^{II}-DpaTyrs with D3×2 peptides by using fluorescence quenching titration. We initially examined the titration between the monomer complex **1**-2Ni^{II} and AMCA-D3 peptide having a fluorescent coumarin unit (AMCA) at the adjacent Lys residue (Figure 3). When **1**-2Ni^{II} was added to the aqueous solution of AMCA-D3 peptide (1 μM in 50 mM HEPES, 100 mM NaCl, pH 7.2), the fluorescence assigned to the AMCA unit decreased to ≈30% of its original intensity (Figure 4a). The change of the fluorescence intensity at 450 nm was evaluated by curve fitting analysis to afford $K_{app} = 3.1 \times 10^5$ M^{-1}. This value is almost the same as that observed in the ITC experiment between **1**-2Ni^{II} and D3 peptide ($K_{app} = 1.5 \times 10^5$ M^{-1}), this validates the fluorescence quenching titration for the binding analysis. A significant fluorescence quenching was also observed in the titration between the Ni^{II}-DpaTyr dimer (**4**-4Ni^{II}) and AMCA-D3-NG-D3 peptide. However, the sharp decrease of fluorescence intensity prevented the precise evaluation of the binding affinity (data not shown). Thus, the titration was next carried out in the presence of an excess amount of **4**-4Zn^{II} as a competitive binder, the bind-

AMCA-D3 : Ac-K(ε-AMCA)-ADDDA-NH$_2$
AMCA-D3-NG-D3 : Ac-K(ε-AMCA)-ADDDNGDDDA-NH$_2$
AMCA-D3-PG-D3 : Ac-K(ε-AMCA)-ADDDPGDDDA-NH$_2$
AMCA-D3-AA-D3 : Ac-K(ε-AMCA)-ADDDAADDDA-NH$_2$

AMCA =

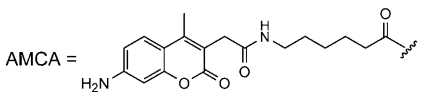

Figure 3. Sequences of the AMCA-labeled oligo-aspartate peptides.

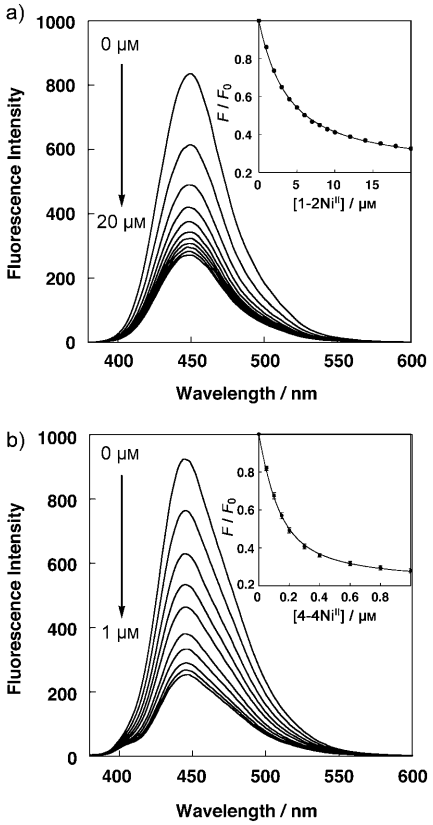

Figure 4. Fluorescence quenching titration of the AMCA-labeled oligo-aspartate peptide with the Ni^{II}-DpaTyr complex. a) Fluorescence spectral change of AMCA-D3 peptide (1 μM) upon addition of **1**-2Ni^{II} (0–20 μM). Inset: curve-fitting analysis of the fluorescence emission change at 450 nm. b) Fluorescence spectral change of AMCA-D3-NG-D3 peptide (0.1 μM) upon addition of **4**-4Ni^{II} (0–1.0 μM) in the presence of 10 μM of **4**-4Zn^{II}. Inset: curve-fitting analysis of the fluorescence emission change at 450 nm. Measurement conditions: 50 mM HEPES, 100 mM NaCl, pH 7.2, 25 °C.

ing affinity of which, for the AMCA-D3-NG-D3 peptide, was readily determined by non-competitive titration under the same conditions (Table 4, Figure S1 in the Supporting Information). When **4**-4Ni^{II} was added to the aqueous solution of AMCA-D3-NG-D3 peptide (0.1 μM in 50 mM HEPES, 100 mM NaCl, pH 7.2) in the presence of a large excess of **4**-4Zn^{II} (10 μM), a significant fluorescence decrease

Table 4. Summary of the binding constants (K_{app}, M^{-1}) of **1**-2Ni^{II} or **1**-2Zn^{II} for various oligo-aspartate peptides determined by the fluorescence titration.[a,b]

	2-4Ni^{II}	**3**-4Ni^{II}	**4**-4Ni^{II}	**4**-4Zn^{II}
AMCA-D3-NG-D3	8.5×10^{8}	1.7×10^{9}	2.0×10^{9}	1.5×10^{7}
	(5.6×10^{6})	(1.1×10^{7})	(1.3×10^{7})	
AMCA-D3-PG-D3	1.1×10^{9}	1.6×10^{9}	1.8×10^{9}	1.1×10^{7}
	(9.5×10^{6})	(1.3×10^{7})	(1.6×10^{7})	
AMCA-D3-AA-D3	4.9×10^{8}	7.7×10^{8}	8.9×10^{8}	1.1×10^{7}
	(4.4×10^{6})	(6.9×10^{6})	(8.1×10^{6})	

[a] Measurement conditions: 50 mM HEPES, 100 mM NaCl, pH 7.2, 25 °C. [b] The binding constants in the parentheses are the apparent values directly obtained by the competitive titration in the presence of 10 μM of **4**-4Zn^{II}.

was again observed as shown in Figure 4b. The titration curve showed a typical saturation manner, and the curve fitting analysis afforded $K_{app}=1.3\times10^{7}\,M^{-1}$. This value was further analyzed based on the competitive binding equation to afford $K_{app}=2.0\times10^{9}\,M^{-1}$ as a binding constant between **4**-4Ni^{II} and AMCA-D3-NG-D3.[13] This value is $\approx10^{4}$-fold larger than the binding between the monomeric **1**-2Ni^{II} and D3 peptide ($K_{app}=3.1\times10^{5}\,M^{-1}$ determined from the fluorescence titration), clearly indicating that the multivalent coordination between the polyaspartate residues of the tag and the tetranuclear Ni^{II} centers of the probe works effectively to enhance the binding affinity. It is of particular importance that this binding affinity ($K_{app}=2.0\times10^{9}\,M^{-1}$) is ≈130-fold greater than that of the corresponding binding between the dimeric Zn^{II} complex **4**-4Zn^{II} ($K_{app}=1.8\times10^{7}\,M^{-1}$) and D4×2 peptide (DDDDGDDDD), which is an optimal tag-probe pair previously reported by us.[8a] The binding constants of the series of the dimer complexes towards the three different D3×2 peptides are summarized in Table 4. It is generally shown that the Ni^{II} complexes are stronger by ≈50–160-fold in the binding affinity, relative to the corresponding Zn^{II} complex in all cases. Among them, the interaction between **4**-4Ni^{II} and AMCA-D3-NG-D3 is the best pair, displaying the strongest binding affinity ($K_{app}=2.0\times10^{9}\,M^{-1}$), though the binding constant is not significantly affected by the structure of the Ni^{II} complex and the tag sequence ($K_{app}=2.0$–$0.49\times10^{9}\,M^{-1}$). This might be ascribed to the relatively flexible structure of both tag and probe, which allows them to adopt suitable conformations for the binding.

The validity of the pair of **4**-4Ni^{II} and D3×2 tag was further evaluated on a protein surface by using FKBP12 (FK506 binding protein 12) that has a D3×2 tag (DDDNGDDD) at its *N*-terminal. To determine the binding affinity by the fluorescence quenching experiment, a fluorophore-appended FKBP12 protein (Flu-D3×2-FKBP12) was prepared by the Michael-type reaction between fluorescein 5-maleimide and a cysteine introduced at the neighboring site of the D3×2 tag. When **4**-4Ni^{II} was added to the PBS buffer solution (10 mM phosphate buffer, 138 mM NaCl, 2.7 mM KCl, pH 7.4) of Flu-D3×2-FKBP12 (0.05 μM), a sharp and significant decrease of the fluorescence took place (Figure 5a, b). The change of the fluorescence intensity was analyzed by curve-fitting analysis to afford $5\times10^{8}\,M^{-1}$ as a binding constant, the value of which is comparable to that with the AMCA-appended peptides (Table 4). As a control experiment, the titration using the fluorescein-appended FKBP12 protein lacking a D3×2 tag (Flu-FKBP12) was conducted, showing only a slight decrease of the fluorescence (Figure 5b). These results clearly demonstrate that the pair of **4**-4Ni^{II} and D3-NG-D3 tag works effectively in the selective binding of a D3×2-tag-fused protein.

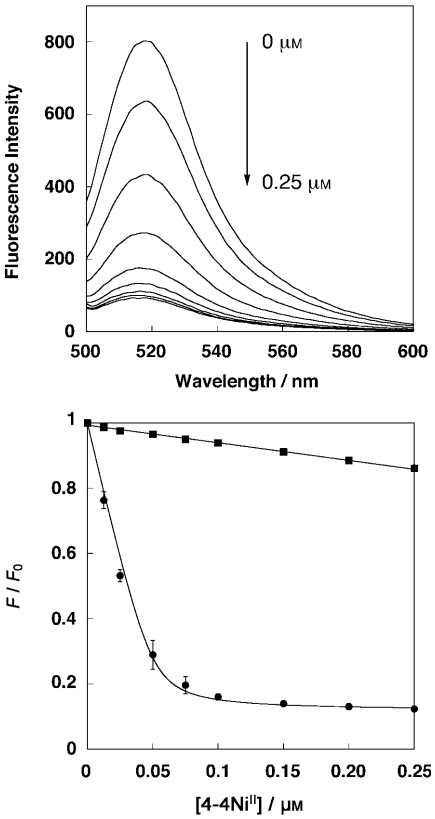

Figure 5. a) Fluorescence spectral change of the fluorescein labeled FKBP12 protein tethered with a D3×2 tag (Flu-D3×2-FKBP12, 0.05 μM) upon addition of **4**-4Ni^{II} (0–0.25 μM). b) Plot of the fluorescence emission change at 518 nm observed in the titration of Flu-D3×2-FKBP12 (●) or Flu-FKBP12 lacking a D3×2 tag (■) with **4**-4Ni^{II}. Measurement conditions: PBS buffer (10 mM phosphate buffer, 138 mM NaCl, 2.7 mM KCl, pH 7.4), 25 °C.

Inactivation of a Tag-Fused Protein by Using the CALI Technique

CALI is a technique that enables the selective inactivation of a protein of interest for elucidation of its biological function through a loss of function process.[14] Strong light irradiation to the chromophore (photosensitizer) generates short-lived reactive oxygen species, such as singlet oxygen that can inactivate a protein in the immediate vicinity of the chromophore. Recently, several successful examples of CALI studies have been reported by using various protein-labeling techniques.[15] To demonstrate the utility of the present tag/probe pair in biological research, we examined the CALI experiment by using a photosensitizer-appended Ni^{II}-DpaTyr probe. Figure 6 illustrates the schematic representation of the CALI experiment, in which the selective binding of the photosensitizer-appended Ni^{II}-DpaTyr to a D3NGD3 tag should facilitate an inactivation of the tag-fused protein by the action of light irradiation.

A new Ni^{II}-DpaTyr probe (**5**-4Ni^{II}) was designed for the CALI experiment, as shown in Figure 6. **5**-4Ni^{II} possesses diiodo-BODIPY (4,4′-difluoro-4-bora-3a,4a-diaza-*s*-indecene) as a photosensitizer unit,[15] which was separated from the Ni^{II}-DpaTyr unit through a rigid linker unit to prevent unfavorable intramolecular interactions between the two units. The synthesis of **5**-4Ni^{II} is outlined in Scheme 1. Briefly, the sequential conjugation reactions between the linker unit **6** and **7**, and between **9** and **10** gave the DpaTyr dimer **11**. The hydrogenation of the azide group of **11** was followed by the conjugation reaction with the activated ester of diiodo-BODIPY **12**[15] to yield the ligand **5**. The complexation of **5** with 4 equiv of $Ni^{II}Cl_2$ in aqueous solution provided the CALI probe **5**-4Ni^{II}. We employed β-galactosidase as a model target protein, which was fused with a D3×2 tag (DDDNGDDD) at its *N*-terminal. The mixture of the lysate of *E.coli* BL21 star™(DE3) expressing the D3×2-tag-fused β-galactosidase and **5**-4Ni^{II} was irradiated with a mercury lamp (510–550 nm), and the CALI efficiency was evaluated based on the hydrolysis activity of the β-galactosidase by using ONPG (*o*-nitrophenyl-β-galactopyranoside) as a substrate. As shown in Figure 7a, the rapid inactivation of the tag-fused β-galactosidase took place by the presence of **5**-4Ni^{II}, wherein the inactivation rate increased by the elongation of the irradiation time to reach to 73% after 5 min. This is a good contrast to the CALI experiment using the β-galactosidase lacking a D3×2 tag, wherein the inactivation rate was only 27% after 5 min. These results clearly indicate that the tag-probe interaction largely enhances the CALI efficiency, as a result of the immediate vicinity of the diiodo-BODIPY unit to the tag-fused β-galactosidase. Several control experiments were further carried out to confirm that the inactivation of β-galactosidase is actually induced by the CALI process (Figure 7b). First, negligible inactivation rate (3%) was observed without light irradiation. Second, the inactivation rate significantly decreased to 9% and 25% when the irradiation was conducted without **5**-4Ni^{II} and with **4**-4Ni^{II} lacking a diiodo-BODIPY unit, respectively. Finally, the addition of 20 mM sodium azide, a well-known singlet oxygen quencher, largely suppressed the inactivation rate to 29%, further supporting that the light-induced formation of the reactive oxygen species mainly contributes to the disruption of the β-galactosidase activity. It is also pointed out that the Zn^{II} complex **5**-4Zn^{II} is less effective (55%) for the enzyme inactivation compared to the corresponding Ni^{II} complex **5**-4Ni^{II} (Figure 7a). Since the inactivation activity of both the Ni^{II}- and Zn^{II}-DpaTyr probe was almost the same when the CALI experiment was conducted using the purified β-galactosidase in the HEPES buffer (80–90% after 5 min irradiation), this result suggests an advantage of the strong binding ability of **5**-4Ni^{II} towards the tag-fused protein, which works more effectively than **5**-4Zn^{II} under crude lysate conditions.

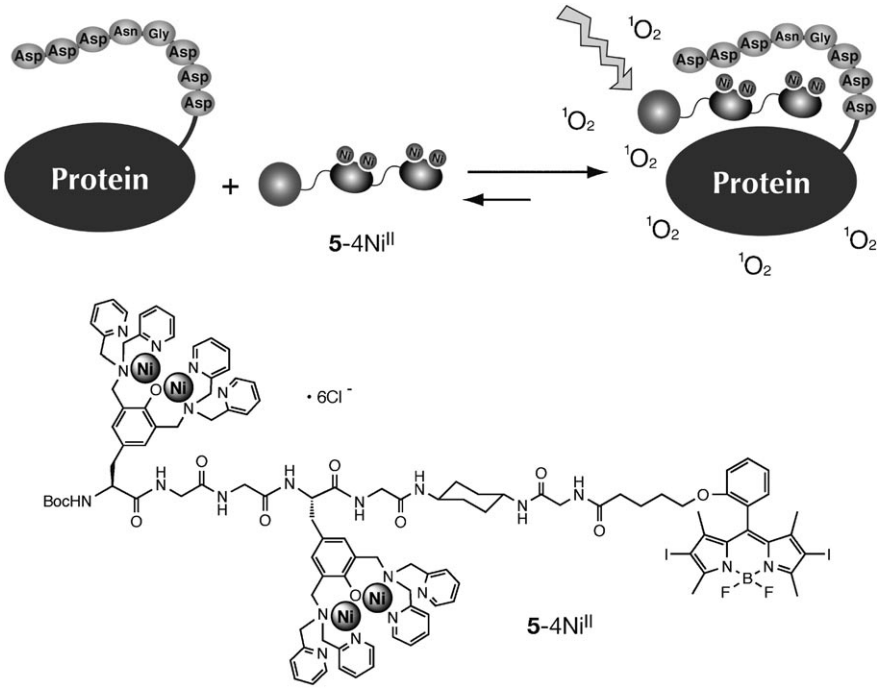

Figure 6. a) Schematic illustration of the CALI (chromophore-assisted light inactivation) experiment using the specific binding pair between **5**-4Ni^{II} and the D3×2-tag-fused protein. b) Structure of the photosensitizer-appended CALI probe **5**-4Ni^{II}.

CHEMISTRY
AN ASIAN JOURNAL

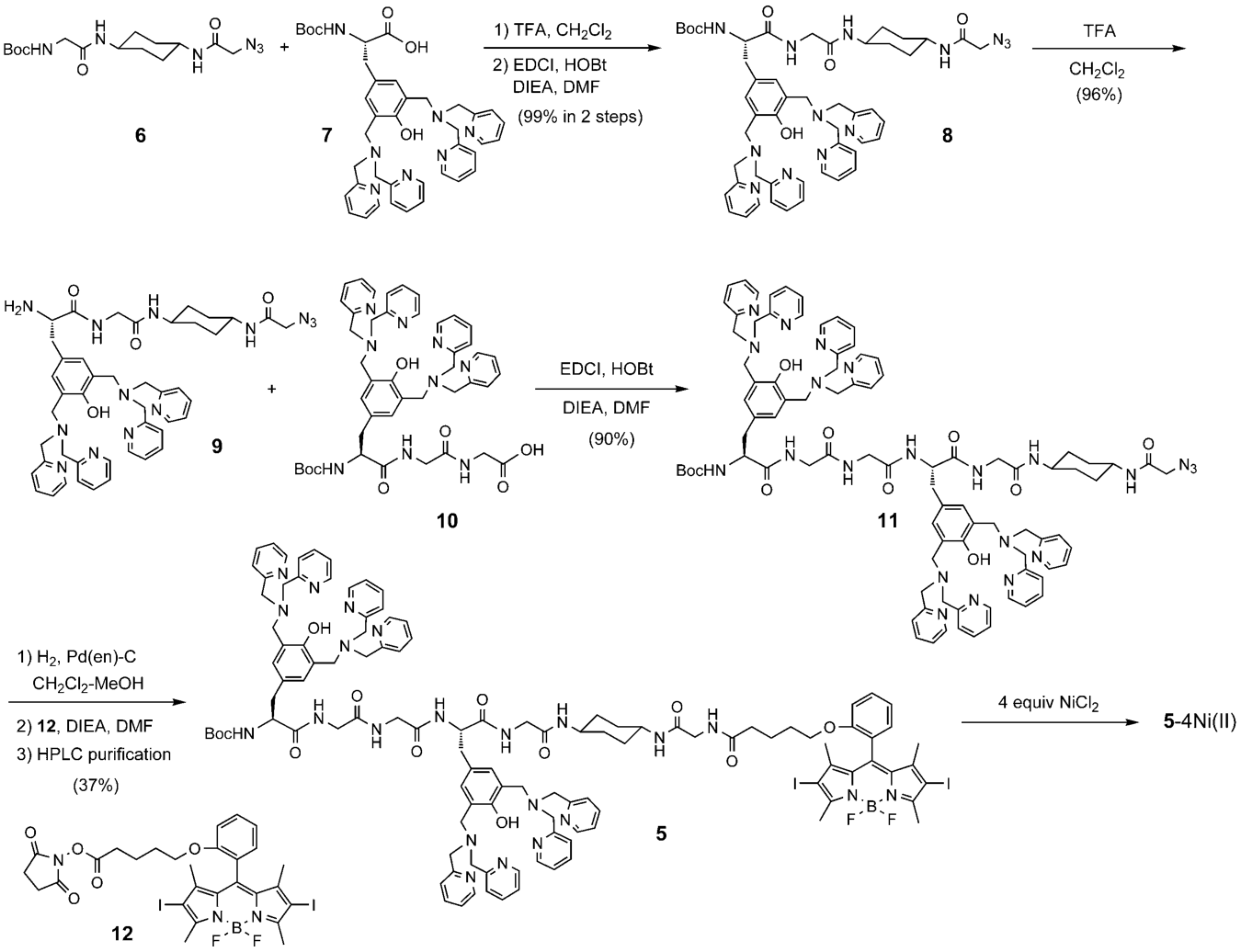

Scheme 1. Synthesis of the CALI probe **5**-4Ni^{II}.

Conclusions

In summary, we have demonstrated that Ni^{II}-DpaTyr is an effective binding probe for the oligo-aspartate tag-fused proteins. The binding constant of the optimized tag-probe pair, i.e., Ni^{II}-DpaTyr dimer **4**-4Ni^{II} and D3×2 tag (DDDNGDDD), reaches to 5×10^{8}–2×10^{9} M^{-1} under neutral aqueous conditions. This binding fully exploits the multiple coordination interaction between the polyaspartate residues of the tag and the tetra-nuclear Ni^{II} centers of the probe, by which the strong affinity was achieved in the molecular recognition between the relatively small molecular probe and the short-peptide tag. The utility of this pair has been successfully demonstrated by the selective deactivation of the D3×2 tag-fused β-galactosidase in the CALI experiment under the conditions of the crude lysate of *E.coli* cells. We envision further biological application using the present tag-probe pair such as in analysis of protein–protein interaction and protein structure formation. Although the fluorescence quenching character of the Ni^{II} ion may limit the utility of the present tag-probe pair in luminescence-based studies, the refinement of the probe structure, such as employment of a longer linker unit[6c] or a fluorophore insusceptible to the quenching effect,[17] would facilitate further biological applications as a result of the improvement of this shortcoming. Our efforts are now ongoing along this line.

Experimental Section

Syntheses of the Metal Complexes of DpaTyr

The metal complexes of DpaTyr **1**-2M (M = Zn^{II}, Ni^{II}, Mn^{II}, Cu^{II}, Cd^{II}, Co^{III}, Fe^{III}) were prepared by the treatment of the ligand **1** with an aqueous solution of MCl_2 (2 equiv) in MeOH at RT, for 30 min. After removal of the solvent by evaporation, the residue was dissolved in distilled H_2O and then lyophilized. The solid was collected by filtration and washed with AcOEt. The solid was dried in vacuo to give a powder. In the case of **1**–2Co^{III}, a complex of DpaTyr with 2 equiv of $CoCl_2$ was oxidized by O_2 bubbling at RT for 1.5 h.[18] The resultant solution was treated by the same procedure to give a purple solid.

Data for **1**-2Zn^{II}: Yield: 91%; FAB-MS: *m/e*: 918 $[M-2Cl]^+$; elemental analysis (%) calcd for $C_{41}H_{46}N_7O_5{\cdot}2Zn{\cdot}3Cl{\cdot}HCl{\cdot}2H_2O$: C 48.02, H 4.91, N 9.56; found: C 47.81, H 4.91, N 9.56.

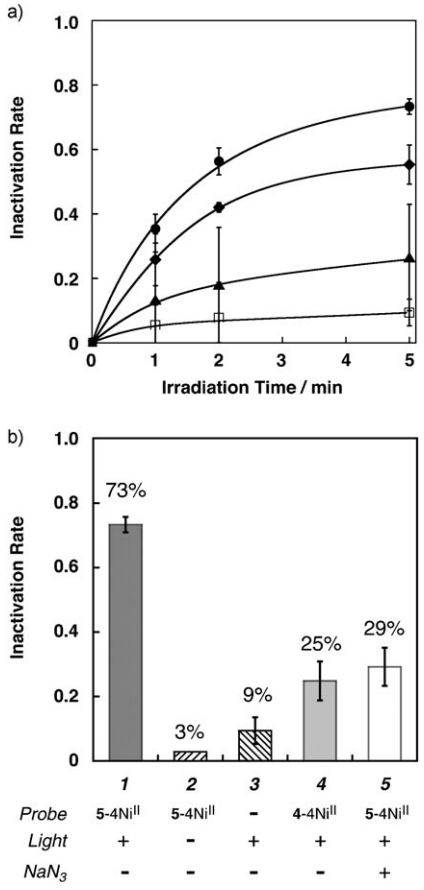

Figure 7. Evaluation of the CALI efficiency for β-galactosidase. a) Time-dependent inactivation of β-galactosidase upon light irradiation. The CALI experiment was performed in the combination of the D3×2 tag-fused β-galactosidase with **5**-4Ni^{II} (●), **5**-4Zn^{II} (◆), or without probe (□), and of the β-galactosidase lacking the D3×2 tag with **5**-4Ni^{II} (▲). b) Summary of the inactivation rate of the β-galactosidase after 5 min of light irradiation under various conditions. The error bars represent standard deviations obtained from at least triplicate experiments. The inactivation rate was defined as $(k_{int,0}-k_{int,irr})/k_{int,0}$, where $k_{int,0}$ and $k_{int,irr}$ is the initial rate of the enzyme reaction observed with the non-irradiated and the irradiated sample, respectively. The detailed experimental conditions are described in the experimental section.

Data for **1**-2Ni^{II}: Yield: 89%; FAB-MS: *m/e*: 902 $[M-2Cl]^+$; elemental analysis (%) calcd for $C_{41}H_{46}N_7O_5{\cdot}2Ni{\cdot}3Cl{\cdot}HCl{\cdot}2H_2O$: C 48.61, H 5.07, N 9.68; found: C 48.49, H 5.13, N 9.73 .

Data for **1**-2Mn^{II}: Yield: 87%; FAB-MS: *m/e*: 896 $[M-2Cl]^+$; elemental analysis (%) calcd for $C_{41}H_{46}N_7O_5{\cdot}2Mn{\cdot}3Cl{\cdot}HCl{\cdot}2H_2O$: C 50.79, H 4.89, N 10.11; found: C 51.03, H 4.73, N 10.15.

Data for **1**-2Cu^{II}: Yield: 94%; FAB-MS: *m/e*: 912 $[M-2Cl]^+$; elemental analysis (%) calcd for $C_{41}H_{46}N_7O_5{\cdot}2Cu{\cdot}3Cl{\cdot}HCl{\cdot}2H_2O$: C 49.90, H 4.80, N 9.94; found: C 50.08, H 4.56, N 9.92.

Data for **1**-2Cd^{II}: Yield: 87%; FAB-MS *m/e*1012 $[M-2Cl]^+$; elemental analysis (%) calcd for $C_{41}H_{46}N_7O_5{\cdot}2Cd{\cdot}3Cl{\cdot}HCl{\cdot}2H_2O$: C 45.41, H 4.37, N 9.04; found: C 45.49, H 4.34, N 9.00.

Data for **1**-2Co^{III}: Yield: 70% in 2 steps; FAB-MS: *m/e*: 904 $[M-2Cl]^+$; elemental analysis (%) calcd for $C_{41}H_{46}N_7O_5{\cdot}2Co{\cdot}4Cl{\cdot}H_2O{\cdot}OH$: C 49.51, H 4.86, N 9.86; found: C 49.90, H 4.76, N 9.98.

Data for **1**-2Fe^{III}: Yield: 73%; FAB-MS: *m/e*: 898 $[M-2Cl]^+$; elemental analysis (%) calcd for $C_{41}H_{46}N_7O_5{\cdot}2Fe{\cdot}5Cl{\cdot}HCl$: C 47.25, H 4.55, N 9.41; found: C 47.31, H 4.65, N 9.13.

Syntheses of the Metal Complexes of the DpaTyr Dimers

The tetranuclear Ni^{II} or Zn^{II} complexes of DpaTyr **2**-4Ni^{II}, **3**-4Ni^{II}, **4**-4Ni^{II}, and **4**-4Zn^{II} were prepared from the corresponding ligands of DpaTyr dimers **2**, **3**, or **4** by complexation with 4 equiv of $NiCl_2$ or $ZnCl_2$ as the same procedure for the synthesis of **1**-2Ni^{II} or **1**-2Zn^{II}. The synthesis of the ligand **2** and **3** was described in the Supporting Information, and the synthesis of **4** was previously reported in the literature.[8a]

Data for **2**-4Ni^{II}: Yield: 94%; FAB-MS: *m/e*: 1713 $[M-3Cl]^+$; elemental analysis (%) calcd for $C_{76}H_{82}N_{14}O_7{\cdot}4Ni{\cdot}6Cl{\cdot}4H_2O{\cdot}2HCl$: C 48.23, H 4.95, N 10.34, found: C 48.19, H 4.79, N 10.35.

Data for **3**-4Ni^{II}: Yield: 94%; FAB-MS: *m/e*: 1770 $[M-3Cl]^+$; elemental analysis (%) calcd for $C_{78}H_{83}N_{15}O_8{\cdot}4Ni{\cdot}6Cl{\cdot}4H_2O{\cdot}2HCl$: C 48.02, H 4.80, N 10.77; found: C 48.22, H 4.87, N 10.97.

Data for **4**-4Ni^{II}: Yield: 92%; FAB-MS: *m/e*: 1827 $[M-3Cl]^+$; elemental analysis (%) calcd for $C_{80}H_{86}N_{16}O_9{\cdot}4Ni{\cdot}6Cl{\cdot}4H_2O{\cdot}2HCl$: C 47.85, H 4.82, N 11.16; found: C 47.87, H 4.84, N 11.26.

Data for **4**-4Zn^{II}: Yield: 87%; FAB-MS: *m/e*: 1845 $[M-3Cl]^+$; elemental analysis (%) calcd for $C_{80}H_{88}N_{16}O_9{\cdot}4Zn{\cdot}6Cl{\cdot}4H_2O{\cdot}2HCl$: C 47.22, H 4.76, N 11.01; found: C 47.00, H 4.53, N 10.91.

*Synthesis of the CALI Probe **5**–4Ni^{II}*

The synthesis was carried out according to the synthetic route shown in Scheme 1. The preparation of **6** is described in the Supporting Information.

Synthesis of **8**: To an ice-cooled solution of **6** (240 mg, 0.68 mmol) in anhydrous CH_2Cl_2 (5 mL) was added dropwise trifluoroacetic acid (5 mL), and the mixture was stirred for 30 min at RT. After removal of the solvent in vacuo, the residue was diluted with water. The aqueous solution was neutralized with aq. NH_3 solution in an ice-bath and then extracted with CH_2Cl_2 (×2). The combined organic layers were dried over Na_2SO_4 and concentrated in vacuo to give the crude amino derivative of **6** as a colorless solid. This crude material used for the next reaction without further purification. A mixture of the crude amine, **7**[8a] (619 mg, 0.88 mmol), EDCI·HCl (EDCI=*N,N*-diisopropylethylamine) (196 mg, 1.02 mmol), HOBt·H_2O (156 mg, 1.02 mmol), and DIEA (DIEA=1-ethyl-3-(3-dimethylaminopropyl)carbodiimide) (0.71 mL, 4.08 mmol) in anhydrous DMF (10 mL) was stirred for 5 h at RT. After dilution with AcOEt, the mixture was washed with sat. $NaHCO_3$ (×2) and brine followed by drying over Na_2SO_4. After removal of the solvent by evaporation, the residue was purified by flash column chromatography on SiO_2 (CH_2Cl_2/MeOH/NH_3; 300:10:1→200:10:1) to give **8** (631 mg, 99%) as a colorless amorphous powder. ^{1}H NMR (400 MHz, $CHCl_3$): δ=11.12 (br s 1H), 8.58 (dd, J=4.8, 0.8 Hz, 4H), 8.39 (br s, 1H), 7.64 (ddd, J=8.0, 7.4, 1.6 Hz, 4H), 7.44 (d, J=8.0 Hz, 4H), 7.16 (ddd, J=7.4, 4.8, 1.2 Hz, 4H), 6.99 (s, 2H), 6.85 (br d, J=8.0 Hz, 1H), 6.08 (d, J=8.0 Hz, 1H), 5.28 (d, J=5.6 Hz, 1H), 4.35–4.30 (m, 1H), 3.98–3.89 (m, 4H), 3.95 (s, 2H), 3.89 (d, J=14.6 Hz, 4H), 3.82 (d, J=14.6 Hz, 4H), 3.75–3.60 (m, 2H), 3.68 (d, J=14.0 Hz, 2H), 3.27 (br d, J=13.2 Hz, 1H), 2.96 (dd, J=13.6, 6.0 Hz, 1H), 2.86 (dd, J=13.6, 9.2 Hz, 1H), 2.00–1.90 (m, 3H), 1.82–1.79 (m, 1H), 1.42 (s, 9H), 1.39–1.15 ppm (m, 4H); FAB-MS: *m/e*: 941 $[M+H]^+$.

Synthesis of **9**: Azide **8** (400 mg, 0.425 mmol) was used as a starting material. According to the same synthetic procedure described for the deprotection of **6**, azide **9** was obtained as a colorless amorphous powder (343 mg, 90%). ^{1}H NMR (400 MHz, $CHCl_3$): δ=11.08 (br s, 1H), 8.52 (ddd, J=5.0, 2.0, 0.8 Hz, 4H), 8.02 (t, J=5.8 Hz, 1H), 7.62 (ddd, J=7.6, 7.6, 2.0 Hz, 4H), 7.47 (d, J=7.6 Hz, 4H), 7.13 (ddd, J=7.4, 5.0, 1.4 Hz, 4H), 7.05 (s, 2H), 6.24 (d, J=8.0 Hz, 1H), 6.14 (d, J=8.0 Hz, 1H), 3.96 (s, 2H), 3.86 (s, 6H), 3.82 (d, J=13.6 Hz, 4H), 3.77 (d, J=13.6 Hz, 4H), 3.74–3.69 (m, 2H), 3.58 (dd, J=9.0, 4.6 Hz, 1H), 3.11 (dd, J=13.8, 4.6 Hz, 1H), 2.60 (dd, J=13.4, 9.0 Hz, 1H), 1.99 (br d, J=6.8 Hz, 4H), 1.34–1.21 ppm (m, 4H); FAB-MS: *m/e*: 1540 $[M+H]^+$.

Synthesis of **11**: A mixture of **9** (150 mg, 0.18 mmol), **10** (175 mg, 0.21 mmol), EDCI·HCl (51 mg, 0.27 mmol), HOBt·H_2O (41 mg, 0.27 mmol), and DIEA (93 μL, 0.53 mmol) in anhydrous DMF (5 mL) was stirred for 4 h at RT. After dilution with AcOEt, the mixture was washed with sat. $NaHCO_3$ (×2) and brine followed by drying over Na_2SO_4. After removal of the solvent by evaporation, the solid was

washed with AcOEt/hexane (1:2) and collected by filtration to give **11** (262 mg, 90%) as a colorless powder. ^{1}H NMR (400 MHz, $CHCl_3$): δ = 11.10 (brs, 2H), 8.88 (brs, 1H), 8.55–8.53 (m, 8H), 8.47 (brs, 1H), 8.29 (brs, 1H), 7.64 (dd, J = 7.6, 2.0 Hz, 4H), 7.60 (dd, J = 7.6, 2.0 Hz, 4H), 7.48 (d, J = 8.0 Hz, 4H), 7.44 (d, J = 8.0 Hz, 4H), 7.19–7.12 (m, 10H), 7.00 (s, 2H), 6.98 (brs, 1H), 6.18 (d, J = 8.0 Hz, 1H), 5.88 (brs, 1H), 4.47 (dd, J = 14.2, 7.4 Hz, 1H), 4.44–4.38 (brm, 1H), 3.99–3.63 (m, 33H), 3.55 (brd, J = 12.8 Hz, 1H), 3.40 (br d, J = 12.8 Hz, 1H), 3.21 (dd, J = 13.8, 7.4 Hz, 1H), 3.04 (dd, J = 13.6, 8.4 Hz, 1H), 2.98–2.88 (m, 2H), 1.95 (brd, J = 10.4 Hz, 4H), 1.49–1.18 (m 4H), 1.32 ppm (s, 9H); FAB-MS: *m/e*: 1640 $[M+H]^+$.

Synthesis of **5**: A solution of **11** (34 mg, 21 μmol) and 10% Pd–C ethylenediamine complex (10 mg) in MeOH–CH_2Cl_2 (1:1, 4 mL) was vigorously stirred for 8 h under H_2 atmosphere at RT. Pd–C was filtered off and washed with MeOH. The filtrate was concentrated in vacuo to give the amino derivative of **11** (31 mg) as a pale yellow amorphous powder. This material was used for the next reaction without further purification; FAB-MS: *m/e*: 1614 $[M+H]^+$.

A solution of the crude amine (11 mg, 6.8 mmol), **12**[15] (7.6 mg, 9.9 μmol), and DIEA (10 μL, 57 μmol) in anhydrous DMF (1 mL) was stirred for 10 hr at RT. The reaction mixture was directly purified by using reverse-phase HPLC (YMC-pack ODS-A, 20×250 mm) with CH_3CN (0.1% TFA)/H_2O (0.1% TFA) solvent system (linear gradient) mode to give **5** (9.9 mg, 63%) as a reddish powder. ^{1}H NMR (400 MHz, $CDCl_3OD$): δ = 8.63 (m, 8H), 7.93 (m, 8H), 7.53–7.48 (m, 17H), 7.17–7.14 (m, 7H), 4.46–4.38 (m, 1H), 4.37 (s, 8H), 4.34 (s, 8H), 4.27 (dd, J = 9.0 5.8 Hz, 1H), 4.23–4.09 (m, 6H), 4.03 (t, J = 6.0 Hz, 2H), 3.88 (dd, J = 16.8, 6.8 Hz, 1H), 3.82–3.56 (m, 11H), 3.07 (dd, J = 14.0, 5.2 Hz, 2H), 2.91 (dd, J = 14.0, 8.8 Hz, 1H), 2.75 (dd, J = 13.8, 9.4 Hz, 1H), 2.54 (s, 6H), 2.10 (t, J = 7.2 Hz, 2H), 1.87–1.79 (m, 4H), 1.66–1.60 (m, 2H), 1.52–1.46 (m, 8H), 1.38–1.25 (m, 4H), 1.18 ppm (s, 9H); FAB-HRMS: *m/e*: calcd for $C_{112}H_{128}BF_2I_2N_{22}O_{12}$ $[M+H]^+$ 2287.8227, found 2287.8213.

Isothermal Titration Calorimetry (ITC) Measurements

ITC titration was performed by using an isothermal titration calorimeter (MicroCal Inc). All measurements were conducted at 298 K. A solution of the peptide (2.0 mM) in a buffer solution (50 mM HEPES, 100 mM NaCl, pH 7.2) was injected stepwise (5 μL×48 times) to a solution of the metal complex of DpaTyr (50 μM) in the same solvent system. The measured heat flow was recorded as function of time and converted into enthalpies (ΔH) by integration of the appropriate reaction peaks. Dilution effects were corrected for by subtracting the result of a blank experiment with an injection of the HEPES solution into cell under identical experimental conditions. The binding parameters (K_{app}, ΔH, ΔS, n) were evaluated by applying one site model using the software Origin (MicroCal Inc.).

Fluorescence Titration with the AMCA-Appended Peptides

The fluorescence spectra were recorded by using a Perkin–Elmer LS55 spectrofluorophotometer. The titration experiments of Ni^{II} or Zn^{II}-DpaTyrs were performed at 25°C using a solution of the AMCA-appended oligo-aspartate peptide in buffer solution (50 mM HEPES, 100 mM NaCl, pH 7.2) in a quartz cell. The concentration of the AMCA-appended peptide was determined based on the reported extinction coefficient of AMCA-X, SE (ε = 19,000 $cm^{-1}M^{-1}$, Invitrogen). The competitive titrations of the tetranuclear Ni^{II}-complex were performed in the presence of 10 μM of **4**–4Zn^{II} in a buffer solution (50 mM HEPES, 100 mM NaCl, pH 7.2) of the AMCA-appended peptide (0.1 μM). The fluorescence emission spectra (excitation wavelength; λ_{ex} = 350 nm) were measured immediately after addition of a freshly prepared aqueous solution of Ni^{II}-DpaTyrs with a micro syringe. Fluorescence titration curves (λ_{em} = 450 nm) were analyzed using nonlinear least-square curve-fitting assuming 1:1 binding to evaluate the apparent binding constant (K_{app}, M^{-1}). The binding constants (K_2) of the tetranuclear Ni^{II}-complexes with a series of oligo-aspartate peptides (Table 4) were calculated based on the following Equation (1):

$$K_{app} = \frac{K_2}{1 + K_1[\mathbf{4} - 4\,Zn^{II}]} \quad (1)$$

In which K_1 is the binding constants between **4**–4Zn^{II} and the peptide which was separately obtained by the non-competitive fluorescence titration experiment.

Fluorescence Titration with the Fluorescein-Appended FKBP12

The titration experiments were performed at 25°C using a solution of Flu-(D3×2)-FKBP12 or Flu-FKBP12 in PBS buffer (10 mM phosphate buffer, 138 mM NaCl, 2.7 mM KCl, pH 7.4) in a quartz cell. The concentration of the FKBP was determined in SDS-PAGE by comparison of the CBB band intensity with a standard protein. The fluorescence emission spectra (excitation wavelength; λ_{ex} = 492 nm) were measured immediately after addition of an aqueous solution of **4**-4Ni^{II} with a micro syringe. Fluorescence titration curves (λ_{em} = 518 nm) were analyzed using nonlinear least-square curve-fitting assuming 1:1 binding to evaluate the binding constant (K_{app}, M^{-1}).

Selective Inactivation of the Tag-Fused β-Galactosidase by CALI

The crude cell lysate of *E. coli* BL21 star(DE3) expressing the β-galactosidase fused with a D3×2 tag (DDDNGDDD) was mixed with a DMSO solution **5**-4Ni^{II} (3 μM in final concentration), which was prepared by in situ complexation of **5** with 4 equivalent of Ni^{II} ions by using an aqueous solution of $NiCl_2$ (10 mM). The mixture (55 μL, containing 3% DMSO) was spotted on a 96-well glass-base plate and irradiated for appropriate time with a mercury lamp (100 W) through a bandpass filter (510–550 nm) on the stage of a fluorescence microscope (IX-71, OLYMPUS). The irradiated solution (50 μL) was replaced on a 96-well polystyrene-base plate, and mixed with a solution (50 μL) of *o*-nitrophenyl-ß-galactopyranoside (ONPG) (1.33 mg mL^{-1} in 200 mM sodium phosphate buffer (pH 7.3), 2 mM $MgCl_2$, 100 mM β-mercaptoethanol). The absorbance change at 420 nm was monitored for 2 min at 37°C using a plate reader (Infinite M200, Tecan) to obtain the initial rate of the enzyme reaction. The inactivation rate was defined as the following Equation (2):

$$\text{Inactivation rate} = \frac{k_{int,0} - k_{int,irr}}{k_{int,0}} \quad (2)$$

In which $k_{int,0}$ and $k_{int,irr}$ is the initial rate of the enzyme reaction observed with the non-irradiated and the irradiated sample, respectively.

Acknowledgements

S.F. thanks JSPS for his predoctoral fellowship.

[1] a) N. M. Green, *Methods Enzymol.* **1990**, *184*, 51–67; b) M. Howarth, D. J.-F. Chinnapen, K. Gerrow, P. C. Dorrestein, M. R. Grandy, N. L. Kellher, A. EL-Husseini, A. Y. Ting, *Nat. Methods* **2006**, *3*, 267–273.

[2] a) L. W. Miller, Y. Cai, M. P. Sheetz, V. W. Cornish, *Nat. Methods* **2005**, *2*, 255–257; b) I. Remy, S. W. Michnick, *Proc. Natl. Acad. Sci. USA* **2001**, *98*, 7678–7683; c) D. I. Israel, R. J. Kaufman, *Proc. Natl. Acad. Sci. USA* **1993**, *90*, 4290–4294; d) J. T. Bolin, D. J. Filman, D. A. Matthews, R. C. Hamlin, J. Kraut, *J. Biol. Chem.* **1982**, *257*, 13650–13662.

[3] a) L. A. Banaszynski, C. W. Liu, T. J. Wandless, *J. Am. Chem. Soc.* **2005**, *127*, 4715–4721; b) S. Schlatter, C. Senn, M. Fussenegger, *Biotechnol. Bioeng.* **2003**, *83*, 210–225; c) H. D. Mootz, E. S. Blum, A. B. Tyszkiewicz, T. W. Muir, *J. Am. Chem. Soc.* **2003**, *125*, 10561–10569; d) J. J. Kohler, C. R. Bertozzi, *Chem. Biol.* **2003**, *10*, 1303–1311; e) S. N. Ho, S. R. Bigger, D. M. Spencer, S. L. Schreiber, G. R. Crabtree, *Nature* **1996**, *382*, 822–826; f) V. M. Rivera, T. Clackson, S. Natesan, R. Pollock, J. F. Amara, T. Keenan, S. R. Magari, T. Phillips, N. L. Courage, F. Cerasoli, D. A. Holt, M. Gilman, *Nat. Med.* **1996**, *2*, 1028–1032.

[4] a) M. Fernández-Suárez, A. Y. Ting, *Nat. Rev. Mol. Cell Biol.* **2008**, *9*, 929–943; b) T. L. Halo, J. Appelbaum, E. M. Hobert, D. M. Balkin, A. Schepartz, *J. Am. Chem. Soc.* **2009**, *131*, 438–439; c) K. M. Marks, M. Rosiov, G. P. Nolan, *Chem. Biol.* **2004**, *11*, 347–356; d) B. A. Griffin, S. R. Adams, R. Y. Tsien, *Science* **1998**, *281*, 269–272; e) E. Hochuli, H. Döbeli, A. Schacher, *J. Chromatogr.* **1987**, *411*, 177–184.

[5] a) J. Arnau, C. Lauritzen, G. E. Petersen, J. Pedersen, *Protein Expression Purif.* **2006**, *48*, 1–13; b) K. Tomizaki, K. Usui, H. Mihara, *ChemBioChem* **2005**, *6*, 782–789.

[6] a) M. Kamoto, N. Umezawa, N. Kato, T. Higuchi, *Chem. Eur. J.* **2008**, *14*, 8004–8012; b) C. T. Hauser, R. Y. Tsien, *Proc. Natl. Acad. Sci. USA* **2007**, *104*, 3693–3697; c) S. Lata, M. Gavutis, R. Tampé, J. Piehler, *J. Am. Chem. Soc.* **2006**, *128*, 2365–2372; d) E. G. Guignet, R. Hovius, H. Vogel, *Nat. Biotechnol.* **2004**, *22*, 440–444.

[7] a) M. V. Rekharsky, T. Mori, C. Yang, Y. H. Ko, N. Selvapalam, H. Kim, D. Sobransingh, A. E. Kaifer, S. Liu, L. Isaacs, W. Chen, S. Moghaddam, M. K. Gilson, K. Kim, Y. Inoue, *Proc. Natl. Acad. Sci. USA* **2007**, *104*, 20737–20742; b) I. Hwang, K. Baek, M. Jung, Y. Kim, K. M. Park, D.-W. Lee, N. Selvapalam, K. Kim, *J. Am. Chem. Soc.* **2007**, *129*, 4170–4171.

[8] a) A. Ojida, K. Honda, D. Shinmi, S. Kiyonaka, Y. Mori, I. Hamachi, *J. Am. Chem. Soc.* **2006**, *128*, 10452–10459; b) H. Nonaka, S. Tsukiji, A. Ojida, I. Hamachi, *J. Am. Chem. Soc.* **2007**, *129*, 15777–15779; c) K. Honda, S. Fujishima, A. Ojida, I. Hamachi, *ChemBioChem* **2007**, *8*, 1370–1372; d) K. Honda, E. Nakata, A. Ojida, I. Hamachi, *Chem. Commun.* **2006**, 4024–4026.

[9] The coordination geometry and structure of the binuclear Ni^{II} complex of 2,6-bis(Dpa)-*p*-cresol with two acetate anions were reported by the following manuscript; H. Adams, D. Bradshaw, D. E. Fenton, *Inorg. Chim. Acta* **2002**, *332*, 195–200.

[10] a) A. Ojida, Y. Mito-oka, K. Sada, I. Hamachi, *J. Am. Chem. Soc.* **2004**, *126*, 2454–2463; b) M. Rekharsky, Y. Inoue, S. Tobey, A. Metzger, E. Anslyn, *J. Am. Chem. Soc.* **2002**, *124*, 14959–14967; c) S. Kubik, R. Kirchner, D. Nolting, J. Siedel, *J. Am. Chem. Soc.* **2002**, *124*, 12752–12760.

[11] a) O. Hayashida, M. Uchiyama, *J. Org. Chem.* **2007**, *72*, 610–616; b) S. Lata, A. Reichel, R. Brock, R. Tampé, J. Piehler, *J. Am. Chem. Soc.* **2005**, *127*, 10205–10215.

[12] A. S. Holmes, *Biophys. Chem.* **1993**, *48*, 193–204.

[13] B. W. Sigurskjold, *Anal. Biochem.* **2000**, *277*, 260–266.

[14] a) K. M. Marks, P. D. Braun, G. P. Nolan, *Proc. Natl. Acad. Sci. USA* **2004**, *101*, 9982–9987; b) D. G. Jay, H. Keshishian, *Nature* **1990**, *348*, 548–550; c) D. G. Jay, *Proc. Natl. Acad. Sci. USA* **1988**, *85*, 5454–5458.

[15] a) A. Keppler, J. Ellenberg, *ACS Chem. Biol.* **2009**, *4*, 127–138; b) M. E. Bulina, D. M. Chudakov, O. V. Britanova, Y. G. Yanushevich, D. B. Staroverov, T. V. Chepurnykh, E. M. Merzlyak, M. A. Shkrob, S. Lukyanov, K. A. Lukyanov, *Nat. Biotechnol.* **2006**, *24*, 95–99; c) R. Yan, Y. Xiong, B. Chen, S. Negash, T. C. Squier, M. U. Mayer, *Biochemistry* **2006**, *45*, 4736–4748; d) O. Tour, R. M. Meijer, D. A. Zacharias, S. R. Adams, R. Y. Tsien, *Nat. Biotechnol.* **2003**, *21*, 1505–1508.

[16] a) T. Yogo, Y. Urano, A. Mizushima, H. Sunahara, T. Inoue, K. Hirose, M. Iino, M.; K. Kikuchi, T. Nagano, *Proc. Natl. Acad. Sci. USA* **2008**, *105*, 28–32; K. Kikuchi, T. Nagano, *Proc. Natl. Acad. Sci. USA* **2008**, *105*, 28–32; b) T. Yogo, Y. Urano, Y. Ishitsuka, F. Maniwa, T. Nagano, *J. Am. Chem. Soc.* **2005**, *127*, 12162–12163.

[17] C. R. Goldsmith, J. Jaworski, M. Sheng, S. J. Lippard, *J. Am. Chem. Soc.* **2006**, *128*, 418–419.

[18] J. S. Seo N.-D. Sung, R. C. Hynes, J. Chin, *Inorg. Chem.* **1996**, *35*, 7472–7473.

Received: August 11, 2009
Revised: October 5, 2009
Published online: February 8, 2010

